Successive Interactions of a Shock Wave with Serially Arranged Vortices

Se-Myong Chang*

*School of Mechanical Engineering, College of Engineering, Kunsan National University,
San 68 Miryong-dong, Kunsan-shi, Chonbuk 573-701, Korea*

Keun-Shik Chang

*Department of Aerospace Engineering, Korea Advanced Institute of Science and Technology,
373-1 Kusong-dong, Yusong-gu, Taejon 305-701, Korea*

Navier-Stokes computation based on a new simplified model is proposed to investigate the interactions of a moving shock wave with multiple vortices arranged in the serial manner. This model problem simulates shock-vortexlet interactions at the shear layer of a compressible vortex often observed in the experiment. Applying the Foppl's idea, we extended the Rankin's model generally used for the description of a single vortex to the multi-vortex version. The acoustic pulses accelerated and decelerated are successively generated and propagated from each shock-vortex interaction, which simply explains the genesis of eccentrically diverging acoustic waves appearing in the experimental photograph.

Key Words : Shock-Vortex Interaction, Navier-Stokes Equations, Foppl's Idea, Rankin Vortex Model

Nomenclature

A	: Accelerated shock wave
a	: Speed of sound
$A_1, \cdots, A_5$	: Interactive waves by acceleration
D	: Incident shock in the experiment
D_1, D_2, D_3	: Diverging acoustic waves
I	: Incident shock wave
$I_1, \cdots, I_5$	: Interactive waves by deceleration
M_s	: Shock Mach number $(=U_s/a_\infty)$
$M_{v,max}$	: Maximum flow Mach number $(=U_{max}/A_\infty)$
n	: Number of vortices
p_s	: Static pressure
Δp	: Acoustic pulse pressure $(=p(r_2)-p(r_1))$
r	: Distance from vortex center
r_c	: Radius of vortex core
U_{max}	: Maximum tangential speed
U_s	: Shock speed
V_θ	: Tangential velocity
X	: Interval between vortices
ϕ	: Velocity potential
θ	: Azimuth angle

Subscripts

c	: Vortex center
i	: Index of vortex
∞	: Free stream value

---
* Corresponding Author,
 E-mail : smchang@kunsan.ac.kr
 TEL : +82-63-469-4724; **FAX** : +82-63-469-4727
School of Mechanical Engineering, College of Engineering, Kunsan National University, San 68 Miryong-dong, Kunsan-shi, Chonbuk 573-701, Korea. (Manuscript **Received** January 10, 2003; **Revised** October 2, 2003)

1. Introduction

The shock-vortex interaction radiating quadrupole acoustic pulses has been a popular problem in the field of compressible fluid dynamics and aero-acoustics because it is regarded as a key sound source of jet screech noise and an important material for the understanding of more complicated problems such as shock-boundary layer interactions. Dosanjh and Weeks (1965) experimentally visualized the interaction of a

traveling shock with the Karman vortex street downstream from a cylinder. However, their measurement technique did not satisfy the sufficient resolution to investigate properly the complex wave physics inside the vortex, and therefore their interest is soon directed to a more elementary problem such as the interaction of a planar shock with a completely isolated vortex.

During the last two decades, many papers have introduced various simplified models on shock and single vortex interaction (Ribner, 1985; Ellzey et al., 1995; Chatterjee, 2000). They succeeded to clarify the quadrupolar structure along the wavefront of the disturbed shock wave interacting with a vortex. The sound source inside the vortex core is now fully understood owing to the develpment of high-resolution numerical schemes to solve Euler and Navier-Stokes equations (Inoue and Hattori, 1999; Grasso and Pirozzoli, 2000).

As we now understand more about the shock-single vortex interaction, however, our interest returns to an advanced problem, i.e. shock and multi-vortex interaction, which can be one of the building block of nonlinear interaction between Mach waves and eddies in the compressible turbulent flow: see Liu and Lele (2002), for example.

In this paper, a new conceptual model of the serially arranged multiple vortices is suggested, based on the classical Rankin vortex model and the Foppl's idea. This model imitates the shock-vortexlet interaction at the shear layer of the strong vortex in a previous experimental study of the present authors (Chang and Chang, 2000). When a shock wave impinges on the compressible shear layer, the small vortices generated by Kelvin-Helmholtz instability can interact with the incident shock. The diverging acoustic waves of eccentric shape is regarded as the result of shock-vortexlet interaction. The objective of this study is to develop a proper computational model simplifying the orginal physics.

2. Models

The conservative form Navier-Stokes equations

for light gases are solved with setting the Prandtl number as a constant (0.71) and the viscosity is an ordinary function of local temperature by Sutherland law and Stokes' hypothesis (Chang and Chang, 2002). A conventional TVD (total variation diminishing) method with third order in spatial accuracy and second order in temporal accuracy is used for the numerical investigation of the system of equations (Chang and Chang, 2001). The QUAG (quadrilateral unstructured adaptive grid) technique is applied to obtain a finer resolution on the sharp gradient of waves (Chang et al., 2001).

2.1 Single vortex model

We start from the Rankin vortex model. The tangential velocity profile is defined as

$$
V_\theta = \begin{cases} U_{\max} \dfrac{r}{r_c}, & r \leq r_c \\[2mm] U_{\max} \dfrac{r_c}{r}, & r \geq r_c \end{cases} \tag{1}
$$

The flow field is divided into two regions: the rigid-body rotational core of constant angular speed and the irrotational outer flow. No artificial term is added in Eq. (1) to isolate the vortex from the outer fluid since we found that there is no noticeable precursor interference effect if the initial position of the incident shock wave is farther than $x = -20r_c$. The numerical parasitic wave generated by the vortex-induced flow is not so serious in such a large distance. Other properties can be evaluated from the force equilibrium in the centrifugal direction with the adiabatic or isentropic condition: see the detail in Chang and Lee (2002).

The interactional result of a planar moving shock with the single vortex of Eq. (1) is given in Fig. 1(a)-(d), computed from the experimental condition of Dosanjh and Weeks (1965). The numerical initial conditions are $M_s = 1.29$, $U_{\max} = 177$ m/s, and $r_c = 2.77$ mm, converted to SI units. Fig. 1(a) shows isopycnics at 78 μs after the incident shock passes through the origin or the initial vortex center. This numerical image is equivalent to Fig. 1(b), a Mach-Zehnder interferogram quoted from the original paper of

Dosanjh and Weeks. Fig. 1(c) is the zoomed-in five-level adaptive grids for the capture of Fig. 1(a) instant. The full computational domain of 75 mm×75 mm contains 45,718 nodes and 43,000 elements. Along the two circumferences r_1 and r_2 centered on the vortex in Fig. 1(a), the pressure is sampled versus θ respectively. The difference of two pressures is defined as the a coustic pulse pressure Δp plotted in Fig. 1(d), which shows a good agreement with other mo-

dels : empirical formula of Dosanjh and Weeks (1965), theory of Ribner (1985), and numerical analysis of Ellzey et al.(1995), etc. This graph has four local extremums (a couple of maximum/minimum set), which is a quadrupole.
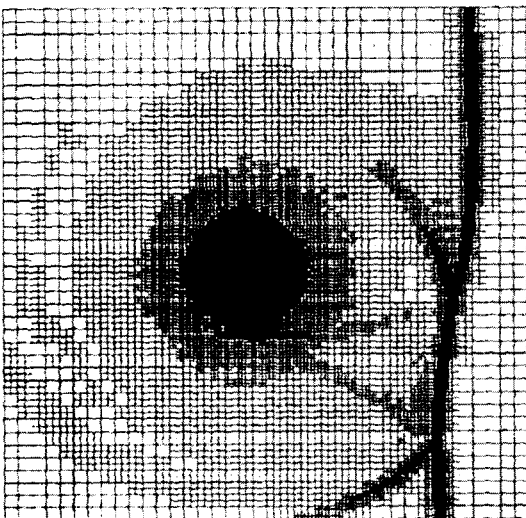
2.2 Multi-vortex model

In the extension of the single vortex model to the multiple vortices, we apply the old idea of Foppl (1913). If each vortex core is treated as
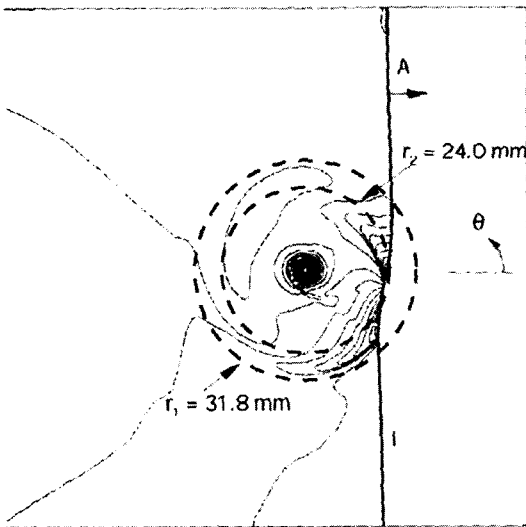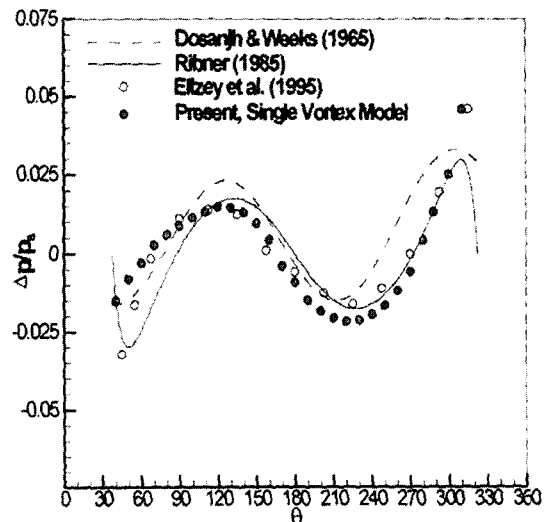

(a) Isopycnics at 78 μs
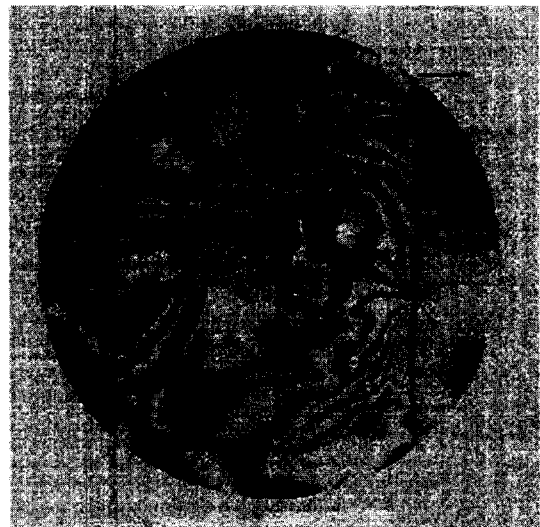
(b) Experimental interferogram, Dosanjh and Weeks (1965)

(c) Quadrilateral unstructured adaptive grid

(d) Quadrupolar pressure distribution

Fig. 1 Shock-single vortex interaction model

singularity, or a concentrated vortex, the irrotational flow field out of the core is determined simply as the sum of all potentials produced by each vortex. Therefore, the effect of every vortex is superposed to calculate the point velocity at the far field; see Fig. 2. This assumption is exactly valid only for the vortex dynamics in ideal flow, but here we extend it to this distributed vorticity case.

The initial distribution inside the core $(r \leq r_c)$ of each vortex is fixed like Eq. (1) because the effect of other vortices is negligible compared with the rotational motion induced by its own vorticity. If the vortex spacing is more than $X = 10r_c$, this assumption becomes more reliable. The tangential velocity at the outer region $(r \geq r_c)$ is given by Foppl's idea

$$V_\theta = \sum_{i=1}^{n} U_{\max} \frac{r_{c,i}}{|r_i|} \qquad (2)$$

where

$$|r_i| = \sqrt{(x - x_{c,i})^2 + (y - y_{c,i})^2}$$

In the classical vortex dynamics, the center of vortex is considered as a sigularity while the outer flow region is irrotational. The superposition of velocity potentials is allowed because the isentropic compressible flow is governed by the following equation:

$$(1 - M_x^2) \frac{\partial^2 \phi}{\partial x^2} + (1 - M_y^2) \frac{\partial^2 \phi}{\partial y^2}$$
$$- 2 M_x M_y \frac{\partial^2 \phi}{\partial x \partial y} = 0 \qquad (3)$$
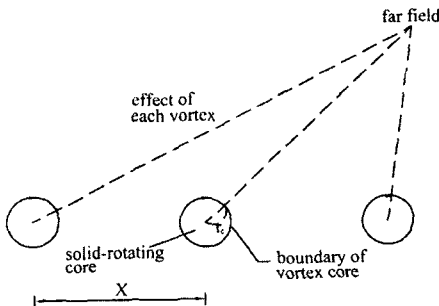

Fig. 2 Schematic of the present multi-vortex model

If the initial background flow is stationary, the Mach numbers $M_x = M_y = 0$. Therefore, Eq. (3) is written down

$$\nabla^2 \phi = 0 \qquad (4)$$

where the irrotational assumption and the method of superposition is valid at least in the initial condition.

From the value of V_θ obtained in Eq. (2), pressure and density distributions can be computed with just several iterations. After a Buckingham's pi analysis, three main parameters for shock and milti-vortex interaction problem are extracted: M_s, $M_{v,\max}$, and X/r_c.

As a representative case, we fix the initial parameters:

$$M_s = 1.5$$
$$M_{v,\max} = 1.0 \qquad (5)$$
$$X/r_c = 20$$

The values listed in Eq. (5) are selected from the similar experiment (Chang and Chang, 2000; Chang et al., 2001). The five vortices $(n = 5)$ are arranged serially on the positive x-axis from the origin, and the incident shock starts from left to right at $x = -20r_c$. The interactive wave patterns are shown in the isopycnics of Fig. 3(a)-(f) where $r_c = 5$ mm.

3. Result and Discussion

3.1 Wave dynamics

The incident shock (I) impinges to five uniform vortices, slightly distorted by the clockwise motion of vortices in Fig. 3(a). In the next Fig. 3(b), the lower half part of I denoted by A is accelerated while the upper half part is captured by the rightest vortex center (I_1). The waves I-I_1 and A-A_1 intersects in a Mach reflection type (Ellzey et al., 1995). This iteraction is sketched schematically in Fig. 4(a), which composes the basis of multiple interactions.

In Fig. 3(c), the decelerated waves (I_1, I_2) and the accelerated shocks (A_1, A_2) are easily discerned after the interaction with two vortices. The outer a wave is located, or the lower sub-
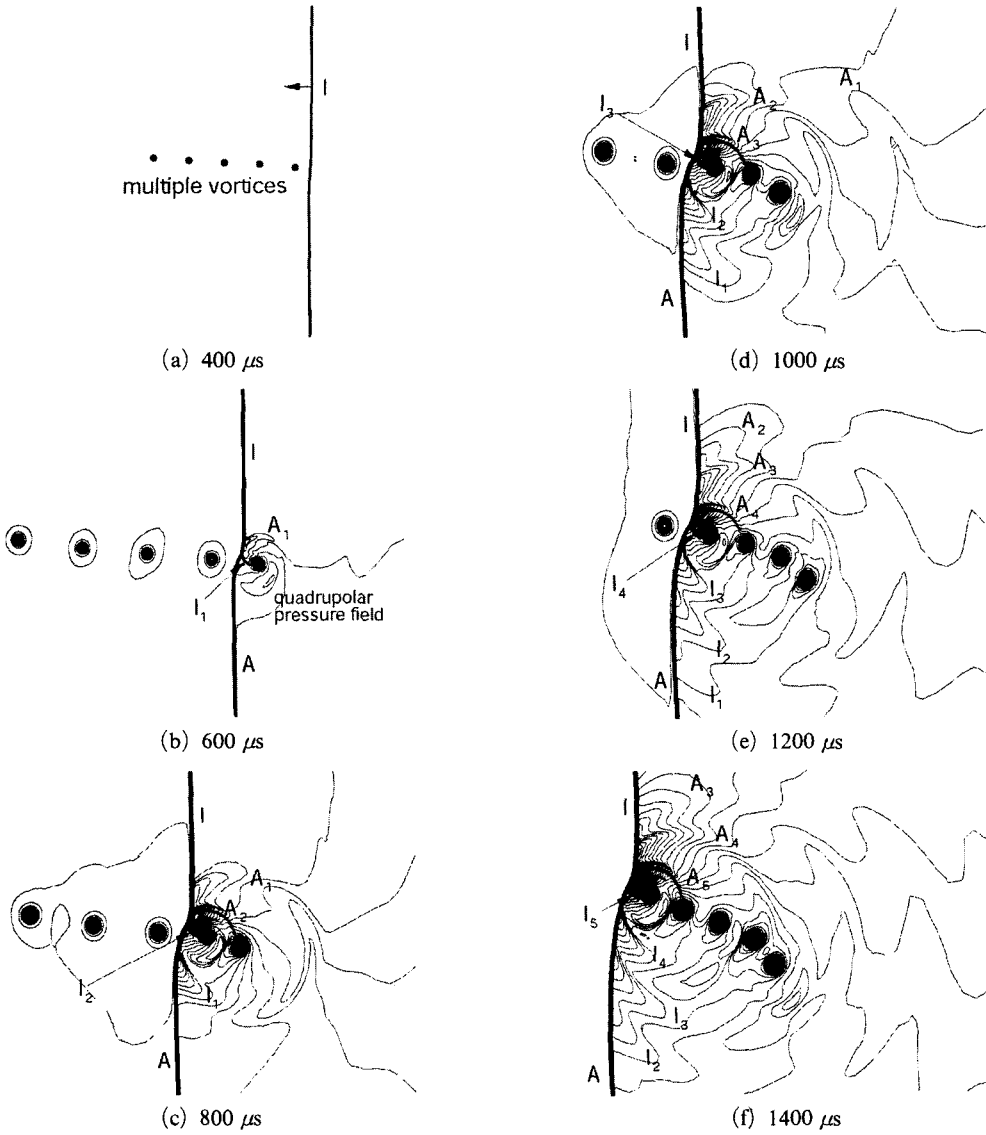
(a) 400 μs

(b) 600 μs

(c) 800 μs

(d) 1000 μs

(e) 1200 μs

(f) 1400 μs

Fig. 3 Interaction of a shock wave with five vortices

(a) Shock-single vortex interaction : see Fig. 3(b)   (b) Shock-multiple vortex interaction : see Fig. 3(f)
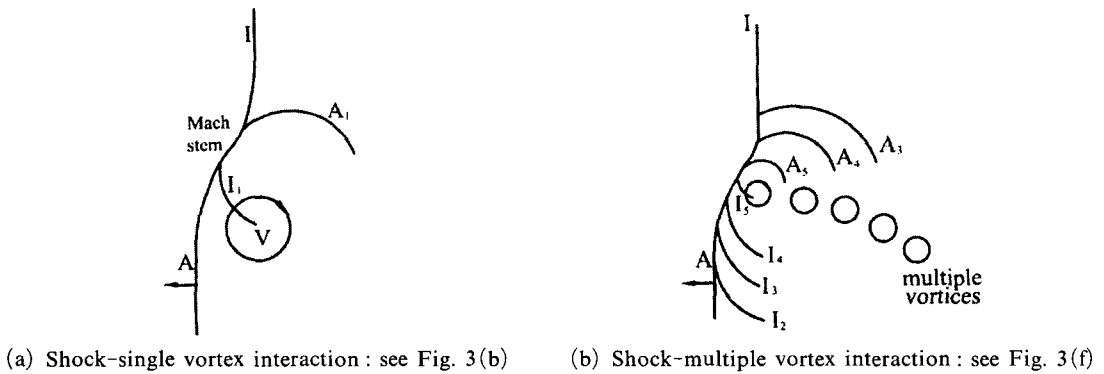
Fig. 4 Schematic of shock-vortex interactions

script mumber indicating that the wave is older, the more rapidly it the smeared, but the vestige still remains in the flow field as wiggled equal density contours. After successive five interactions, the waves I_1, $\cdots$, I_5 and A_1, $\cdots$, A_5 are generated one after another: see Fig. 3(d)–(f). All the speed of propagating waves cannot exceed the incident shock due to the so-called entropy condition, so the accelerated pulses (A_1, $\cdots$, A_5) cannot cross I. This entropy condition is the specific feature of shock and multi–vortex interaction compared with the single vortex case. So they show the attached eccentric pattern like Fig. 4(b). Recall that the vortex array initially placed along the x axis is rotated clockwise by the circulation of the other vortices.

3.2 Comparison with experiment
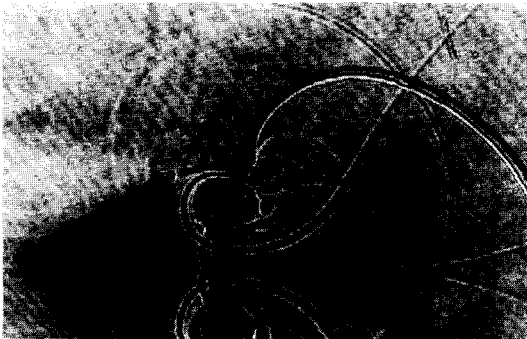
In a shock tube experiment performed by the

Fig. 5 Experimental shadowgraph, Chang and Chang (2000)

present authors, the small vortices are originated from Kelvin–Helmholtz instability at the shear layer of vortex edge (Chang and Chang, 2000). In the shadowgraph of Fig. 5, deverging acoustic waves generated by the interaction of the incident shock and the vortexlets are observed as faint eccentric circles. As shwon in the schematic diagram Fig. 6(a), it seems that the waves D_1, D_2, D_3 are porpagated from vortexlets though they might be ambiguous in Fig. 5 due to the viscous diffusion effect in the shear layer. Fig. 6(a) obviously suggests that the diverging acoustic waves D_1, D_2, D_3 in the experiment should be equivalent to the accelerated waves A_1, A_2, A_3 compared with Fig. 6(b), the sketch for the present numerical study. Then our last question is directed to what is the decelerated pulses I_1, I_2, I_3 in the experiment. Since they are buried in the core of primary vortex, all the decelerated waves are merged to a strong irregular wave at the root of incident shock: see Fig. 5.

4. Conclusion

A computational research based on the new conceptual multi–vortex model is proposed to study the interactive mechanism of the shock wave and serial vortex array. We started from a Rankin's single–vortex model, and extended it by adopting Foppl's idea to the multiple vortex cases. The result of Navier–Stokes *simulation* supports the hypothesis that the diverging acoustic waves in the experiment should be generated

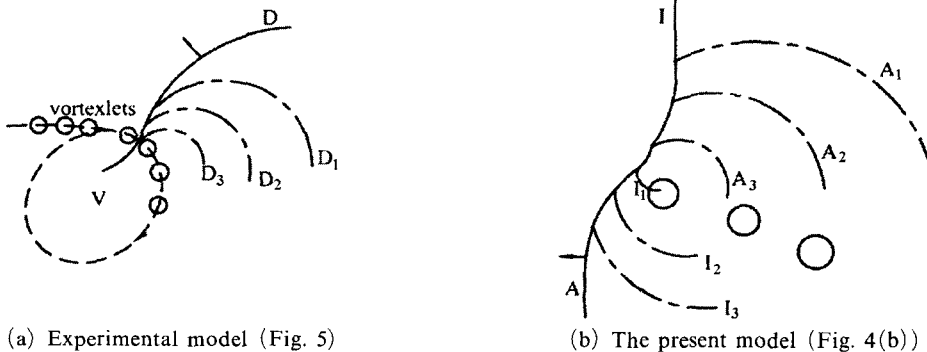(a) Experimental model (Fig. 5)   (b) The present model (Fig. 4(b))

Fig. 6 Comparison of two models

by the shock and small vortices interaction inside the compressible shear layer. Consequently the weak eccentric waves consist of successive accelerated pulses orignating from the interaction of the incident shock with each small vortex.

References

Chang, S. M. and Chang, K. S., 2000, "On the Shock-Vortex Interaction in Schardin's Problem," *Shock Waves*, Vol. 10, No. 5, pp. 333~343.

Chang, S. M., Lee, S. and Chang, K. S., 2001, "Morphological Transformation of Shock Waves Behind a Flat Plate," *KSME International Journal*, Vol. 15, No. 5, pp. 676~682.

Chang, S. M., Chang, K. S., 2001, "Vortex Ring, Shock-Vortex Interaction, and Morphological Transformation Behind a Finite Cone," *KSME International Journal*, Vol. 15, No. 11, pp. 1599~1604.

Chang, S. M. and Chang, K. S., 2002, "Shock Reflection and Penetration Impinging into a Vortex (I) - Experimental Model," *Transactions of KSME* (*B*), Vol. 26, No. 9, pp. 1311~1318.

Chang, S. M. and Lee, S., 2002, "Shock Reflection and Penetration Impinging into a Vortex (II) -Theoretical Model," *Transactions of KSME* (*B*), Vol. 26, No. 9, pp. 1319~1324.

Chatterjee, A., 1999, "Shock Wave Deformation in Shock-Vortex Interactions," *Shock Waves*, Vol. 9, pp. 95~105.

Dosanjh, D. S. and Weeks, T. M., 1965, "Interaction of a Starting Vortex as Well as a Vortex Street with a Travelling Shock Wave," *AIAA Journal*, Vol. 3, pp. 216~223.

Ellzey, J. L., Henneke, M. R., Picone, J. M. and Oran, E. S., 1995, "The Interaction of a Shock with a Vortex : Shock Distortion and the Production of Acoustic Waves," *Physics of Fluids*, Vol. 7, pp. 172~184.

Foppl, L., 1913, "Wirbeibewegung Hinder Einem Kreiszylinder," *Sitz. K. Bayr Akad. Wiss.*, Vol. 1, pp. 7~18.

Grasso, F. and Pirozzoli, S., 2000, "Shock wave-vortex interaction : shock and vortex deformations, and sound production," *Theoretical and Computational Fluid Dynamics*, Vol. 13, pp. 421~456.

Inoue, O. and Hattori, Y., 1999, "Sound Generation by Shock-Vortex Interactions," *Journal of Fluid Mechanics*, Vol. 380, pp. 81~116.

Liu, C. and Lele, S. K., "A Numerical Investigation of Broad-Band Shock Wave," AIAA-2002-0074, 40th AIAA Aerospace Sciences Meeting and Exhibition, 14-17 January 2002, Reno, Nevada, USA.

Ribner, H. S., 1985, "Cylindrical Sound Wave Generated by Shock-Vortex Interaction," *AIAA Journal*, Vol. 23, pp. 1708~1715.